Synergistic effects of drought and deforestation on the resilience of the south-eastern Amazon rainforest

Staal, A., Dekkers, S., Hirota Magalhaes, M., & van Nes, E. H.

Synergistic effects of drought and deforestation on the resilience of the south-eastern Amazon rainforest

Arie Staal[a,b], Stefan C. Dekker[b], Marina Hirota[c], Egbert H. van Nes[a]

[a] Aquatic Ecology and Water Quality Management Group, Wageningen University, P.O. Box 47, 6700 AA, Wageningen, The Netherlands

[b] Department of Environmental Sciences, Copernicus Institute for Sustainable Development, Utrecht University, P.O. Box 80115, 3508 TC Utrecht, The Netherlands

[c] Department of Physics, Federal University of Santa Catarina, P.O. Box 476, 88040-970, Florianópolis, Brazil

Corresponding author: Arie Staal

Phone: +31 317 482689 / Fax: +31 317 484411

E-mail addresses: arie.staal@wur.nl (A. Staal), s.c.dekker@uu.nl (S.C. Dekker), marina.hirota@ufsc.br (M. Hirota), egbert.vannes@wur.nl (E.H. van Nes)

Abstract The south-eastern Amazon rainforest is subject to ongoing deforestation and is expected to become drier due to climate change. Recent analyses of the distribution of tree cover in the tropics show three modes that have been interpreted as representing alternative stable states: forest, savanna and treeless states. This situation implies that a change in environmental conditions, such as in the climate, could cause critical transitions from a forest towards a savanna ecosystem. Shifts to savanna might also occur if perturbations such as deforestation exceed a critical threshold. Recovering the forest would be difficult as the savanna will be stabilized by a feedback between tree cover and fire. Here we explore how environmental changes and perturbations affect the forest by using a simple model with alternative tree-cover states. We focus on the synergistic effects of precipitation reduction and deforestation on the probability of regime shifts in the south-eastern Amazon rainforest. The analysis indicated that in a large part of the south-eastern Amazon basin rainforest and savanna could be two alternative states, although massive forest dieback caused by mean-precipitation reduction alone is unlikely. However, combinations of deforestation and climate change triggered up to 6.6 times as many local regime shifts than the two did separately, causing large permanent forest losses in the studied region. The results emphasize the importance of reducing deforestation rates in order to prevent a climate-induced dieback of the south-eastern Amazon rainforest.

Keywords bistability, climate change, critical transitions, fire, regime shifts, tipping points

1. Introduction

Every year, large areas of rainforest are being deforested in the Amazon. In addition, increased drought is expected to affect parts of the rainforest over the course of the coming century (Malhi et al., 2008). In recent years there has been much interest in the question whether climate change and deforestation may cause the forest to die back, or even collapse due to positive feedbacks that cause alternative stable states (Cox et al., 2000; Lenton et al., 2008; Nepstad et al., 2008; Malhi et al., 2009; Davidson et al., 2012). Analyses of MODIS satellite data of tree cover by Hirota et al. (2011) and Staver et al. (2011b) have added new evidence for alternative states (Scheffer and Carpenter, 2003) by showing that the frequency distributions of tree cover in the tropics have three modes, which roughly correspond to a treeless ecosystem, savanna (tree-grass mosaics) and forest. The probability of finding these modes depends non-linearly on mean annual precipitation (MAP) (Hirota et al., 2011).

The existence of alternative stable states implies that an ecosystem can be in several alternative states under the same external conditions. When the system is perturbed slightly, it will return to the stable equilibrium. However, when a perturbation exceeds a certain size, the system will move to an alternative equilibrium. Such a regime shift can also occur when the environmental conditions cross a fold bifurcation point, often called ‘tipping point’ (Scheffer et al., 2009). Restoring the conditions that were present prior to the shift requires a larger change in environmental conditions, a phenomenon called hysteresis. We refer to these regime shifts as critical transitions (Scheffer, 2009). A slow change in environmental conditions can make a system more vulnerable for a regime shift. The maximum possible perturbation without causing a regime shift is defined by as a system state’s (ecological) resilience (Holling, 1973).

There is increasing evidence that fire is the mechanism for creating alternative stable states of tropical rainforest and savanna (Staver et al., 2011b; Hoffmann et al., 2012; Murphy

and Bowman, 2012). Savannas are open, grassy landscapes, which can be maintained by frequent fires. As fire-exclusion experiments (e.g. Moreira, 2000) have shown, fires can prevent the establishment of forest when the climate would allow for its presence (Bond, 2008). Indeed, the grasses in savannas may fuel natural or anthropogenic fires, which kill forest tree species (Hoffmann et al., 2012). Fires are sometimes seen as external disturbances maintaining an unstable savanna regime (Sankaran et al., 2005). However, fires can be regarded as a self-stabilizing mechanism of savannas, as the low tree cover in savannas enhances fires. Closed-canopy forests, on the other hand, suppress fires through the creation of a humid understory microclimate (Uhl and Kauffman, 1990) and can thereby stabilize the forest state itself (Hoffmann et al., 2012; Murphy and Bowman, 2012). Fragmentation of the canopy results in a much higher vulnerability to fire. Both grasses invading the forest and trees killed by fire can fuel fires, making burned forest areas even more susceptible to burning (Cochrane et al., 1999; Brando et al., 2014). After a number of fires a savanna ecosystem may establish. Next to the internal feedbacks, also climatic conditions influence the probability of fire; the drier it is, the more intense fires tend to be (Pueyo et al., 2010), so the more likely a regime shift from forest to savanna would become. On centennial to millennial time scales, however, these shifts need not be permanent. For an African savanna, for example, back-and-forth transitions between savanna and forest have been reported (Gil-Romera et al., 2010). Such repeated shifting between alternative stable states is called flickering (Scheffer, 2009).

Both deforestation and climate change in the Amazon are relatively severe in the drier, south-eastern part of the basin, an area characterized as the “arc of deforestation” (Aragão et al., 2007; Davidson et al., 2012; Coe et al., 2013). Therefore, in particular tree cover in the south-eastern Amazon can be expected to be out of equilibrium and vulnerable to future regime shifts, but the resilience of the forest is only poorly understood. Our objective was to assess how deforestation (defined as a reduction in tree cover; Sternberg, 2001) and climate

change (a reduction in mean annual precipitation) may interact to induce fire-mediated regime shifts from forest to savanna in the south-eastern Amazon. Current forest models are generally not suited for analyzing tipping point behavior, while there is a need for models that are (Reyer et al., 2015). Previous studies concerned with alternative stable states in the Amazon have mainly focused on a regional forest-precipitation feedback instead of the tree cover-fire feedback (Nobre and Borma, 2009). We present a simple model for tree cover in South America that includes the tree cover-fire feedback and was fitted to near-continent-wide satellite data. We use it to simulate deforestation- and climate change-induced regime shifts to savanna in the south-eastern Amazon rainforest.

2. Methods

2.1. The model

We adapted a simple tree-cover model by Van Nes et al. (2014). It can have three stable tree-cover states, corresponding to treeless, savanna and forest states, and has been fitted to satellite data of tree cover across the Earth's tropics. The model consists of a logistic growth function for the expansion of tree cover T (fraction) to carrying capacity K (fraction) and two loss terms. The expansion rate depends on precipitation P (mm yr^{-1}) and saturates at r_m (yr^{-1}) with a half saturation of h_P (mm yr^{-1}). The first loss term includes increased mortality at low tree-cover densities, called an Allee effect. This represents the facilitative effect of adult trees on tree-seedling establishment in the seedling's competition with grasses (Holmgren et al., 1997; Baudena et al., 2010). The Allee-effect-induced loss rate decreases from m_A (yr^{-1}) with T according to a Monod function with half saturation h_A (fraction). The growth function and Allee effect are given as:

$$\frac{dT}{dt} = \frac{P}{h_P+P}\, r_m\, T\, \left(1 - \frac{T}{K}\right) - m_A\, T\, \frac{h_A}{T+h_A} \quad (1)$$

The Van Nes et al. (2014) model also includes a second mortality term that mimics the effect of fire at intermediate tree cover. A Hill function describes the sigmoidal shape of the negative relationship between tree cover and fire-induced mortality. Thus, fire depends solely on tree cover in Van Nes et al. (2014) and not on environmental conditions. However, in reality fire occurrence and intensity also depend on rainfall (Staver et al., 2011b). Therefore, we adjusted the fire term accordingly for this paper, although we do not depart from the simple approach of Van Nes et al. (2014). In this new model, fire-induced tree-cover mortality depends on fire intensity *I*, whereby trees are resistant to low-intensity fires through a Hill function. Fire intensity depends negatively and non-linearly on tree cover. This can be thought of as representing the availability of fuel (grass), which is determined by the openness of the landscape. Although a fragmented canopy may affect tree cover in several ways (Cumming et al., 2012), this landscape openness mainly promotes the continuity of the grassy (i.e. non-forested) portion of the landscape such that above a certain threshold of this continuity fires can percolate through the landscape (Archibald et al., 2009; Pueyo et al., 2010; Hoffmann et al., 2012; Staver and Levin, 2012). Therefore, *I* depends on a variable landscape continuity *C(T)*, which is a function of tree cover *T* through a saturating sigmoidal function (Hill function). When *T* equals the half saturation h_C the largest change in *C* occurs.

Following the rationale that the moisture content of the fuel, and therefore its flammability, depends on soil moisture (Hirota et al., 2010; Murphy and Bowman, 2012), fire intensity *I* also depends on a soil moisture index *SMI*. This index depends on *P* via a sigmoidal Hill function (Hirota et al., 2010; Staver and Levin, 2012). The choice for a sigmoid is empirically supported by Bucini and Hanan (2007), who found that it could best describe the relationship between mean annual precipitation (MAP) and tree cover in the

139 African savannas. Because our model represents processes on an annual basis, the fire-
140 induced mortality is divided by a constant fire return interval *FRI*. The resulting differential
141 equation for tree cover *T* (fraction) is as follows:
142
143 $$\frac{dT}{dt} = \frac{P}{h_P+P}\, r_m\, T\, \left(1-\frac{T}{K}\right) - m_A\, T\, \frac{h_A}{T+h_A} - T\, \frac{1}{FRI}\, \frac{I(P,T)^\gamma}{h_I{}^\gamma + I(P,T)^\gamma} \quad (2)$$
144
145 with the fire intensity *I(P,T)* (-) defined as:
146
147 $$I(P,T) = C(T) \cdot SMI(P), \quad (3)$$
148
149 landscape continuity *C(T)* (-) as:
150
151 $$C(T) = \frac{h_C{}^\beta}{h_C{}^\beta + T^\beta} \quad (4)$$
152
153 and the soil moisture index *SMI(P)* (-) as:
154
155 $$SMI(P) = \frac{h_{SMI}{}^\alpha}{h_{SMI}{}^\alpha + P^\alpha} \quad (5)$$
156
157 For an explanation of the parameters, see Table 1.
158
159 2.2. Parameterization
160 We fitted the model on tree-cover data for tropical and subtropical South America
161 (13°N−35°S; Fig. 1). We used the data of Hirota et al. (2011). These are average Climate
162 Research Unit (CRU) precipitation data (the average of 1961−2002) at 0.5° resolution

(Mitchell and Jones, 2005) and MODIS Vegetation Continuous Field 3 tree-cover data (31 October 2000 to 9 December 2001) at 0.01° resolution (Hansen et al., 2003). However, we excluded human-used areas and water bodies from the data, as identified in the Global Land Cover 2000 (GLC2000) dataset (classes 16−18 and 20−23; Scheffer et al., 2012), using the R package 'raster'. The probability distributions of tree cover in natural landscapes can be thought of as displaying the interplay between stable attractors and stochasticity in the system (Van Nes et al., 2012). Hence, we assume that fitting the model on the tree-cover modes captures the stable states of the system. To quantify the deviations to these stable states we calculated the adjusted R^2_{model} of the model. Comparing that to the adjusted $R^2_{trimodal}$ of the three means of the modes gives an estimate of how well the model fits the trimodal tree-cover distribution (more details can be found in Appendix A).

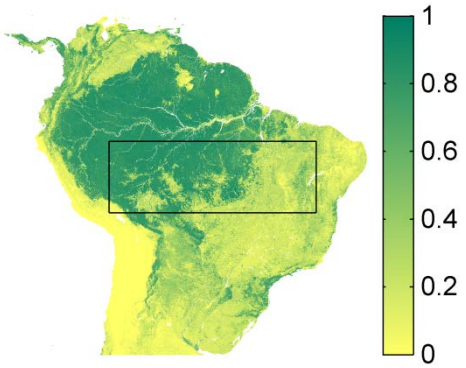

Figure 1: Tree cover (as a fraction) in tropical and subtropical South America. The total area shown was used for parameterizing the model (13°N−35°S, but excluding human-used areas); the study area (5°−15°S, 71°−42°W) is delineated. The data are at 0.01° resolution.

The parameterization of the model (Table 1) was done as follows. The logistic growth function from Van Nes et al. (2014) was kept intact, except for an adjustment of h_P to better match the tree-cover data at low precipitation values. No adjustments were made to the Allee-effect term, because we only fitted on the forest and savanna tree-cover values. In the fire

term, the half saturation for the soil moisture function h_{SMI} was based on Hirota et al. (2010). h_C is interpreted as the unstable threshold in tree cover between savanna and forest and should therefore approximately correspond to the least common tree-cover value between these modes in the South American tree-cover frequency distribution (0.56; Fig. A1). The fire return interval *FRI* was fine-tuned within a realistic range (3−10 years; Ratter, 1992). The remaining parameters, which are half saturation for fire intensity h_I and the exponents α, β and γ were fine-tuned without a predetermined range. This was done such that the model had a forest-savanna bistability range of approximately 1000−2500 mm yr^{-1} (Fig. 2).

Table 1: The model's parameters and their values.

Parameter	Description	Value	Unit	Source
α	Power in soil moisture index function	4	None	Fine-tuning
β	Power in continuity function	6	None	Fine-tuning
γ	Power in fire-induced mortality term	6	None	Fine-tuning
FRI	Fire return interval	7	yr	(Ratter, 1992)
h_A	Half saturation of Allee effect	0.10	Fractional tree cover	(Van Nes et al., 2014)
h_C	Half saturation of grass (non-forest) cover continuity	0.57	Fractional tree cover	This research
h_I	Half saturation of the fire-induced mortality term	0.15	None	Fine-tuning
h_P	Half saturation of growth term	80	mm yr^{-1}	Fine-tuning
h_{SMI}	Half saturation of the soil	1800	mm yr^{-1}	(Hirota et al.,

	moisture index			2010)
K	Maximum tree cover	0.90	Fractional tree cover	(Van Nes et al., 2014)
m_A	Mortality due to Allee effect	0.15	yr^{-1}	(Van Nes et al., 2014)
r_m	Maximum tree-cover growth rate	0.30	yr^{-1}	(Van Nes et al., 2014)

193

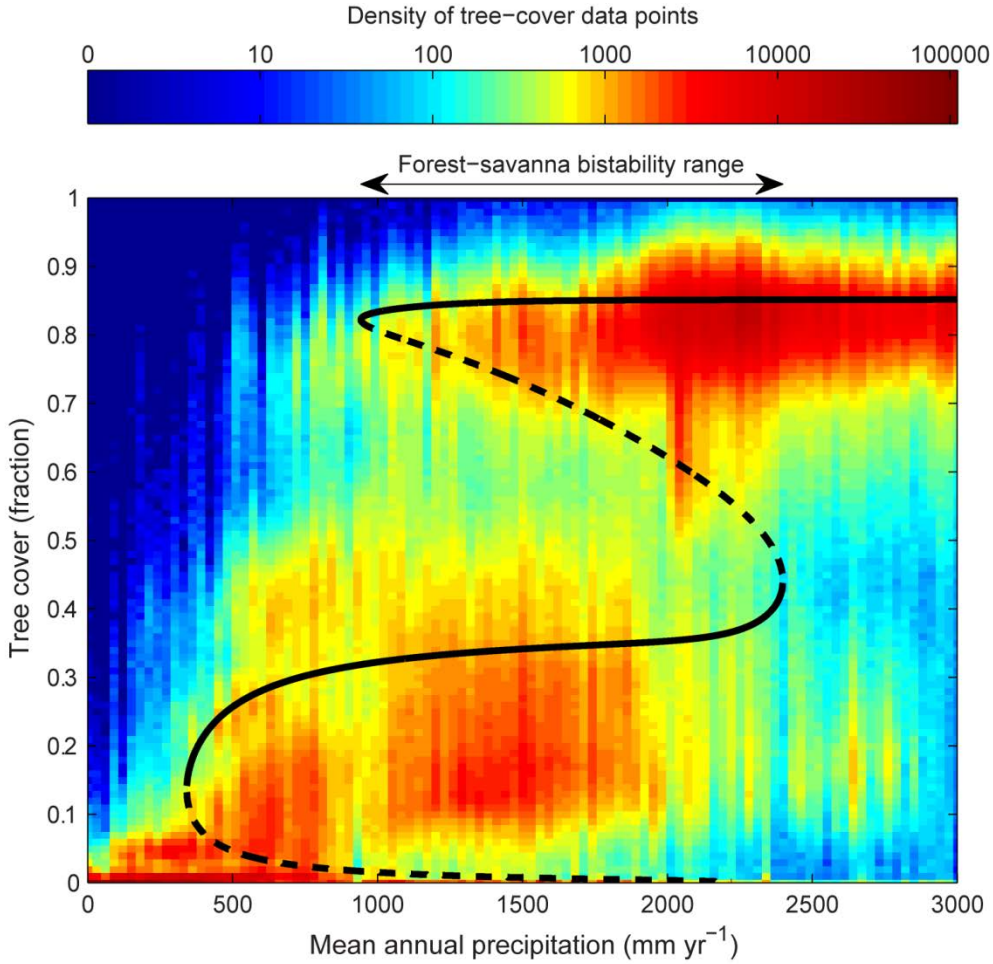

194

195 Figure 2: Equilibria of the model. The stable (solid lines) and unstable (dashed lines)
196 equilibria of the model are shown with the background showing the frequency of tree-cover
197 values from tropical and sub-tropical South America. The data at 0.01° resolution (Hirota et
198 al., 2011) are displayed on a 101 x 101 lattice. Only tree-cover values at locations with MAP

199 up to 3000 mm yr^{-1} are shown (n = 8723784). Note the logarithmic scale along which the
200 distribution of the data are presented.
201
202 2.3. Application
203 The study area to which the model was applied spans 15°−5°S latitude and 71°−42°W
204 longitude (the delineated area in Fig. 1). It mostly covers Brazil, but it also includes the
205 Bolivian part of the Amazon basin and a small part of Peru. This region was chosen to include
206 the forest-savanna boundary in the south-eastern Amazon basin (Hirota et al., 2010) and
207 thereby part of the arc of deforestation, where historical deforestation has been high (Coe et
208 al., 2013). Continued deforestation can be expected for the near future, despite recent and
209 projected increases in protected forest area (Malhi et al., 2008). The region also marks a
210 transition from a dry to a humid tropical climate; an east-west precipitation gradient exists
211 from roughly 800 mm yr^{-1} to 2400 mm yr^{-1} (Fig. A5). Most forest trees belong to evergreen
212 species with limited resistance to fire (Hirota et al., 2010).
213 Because past disturbances have been severe in this region, regional tree cover may be
214 out of equilibrium. As we were interested in how far from equilibrium and how close to a
215 regime shift tree cover in the study area is, we did not exclude human-used areas here. With
216 the unfiltered data we calculated the adjusted R^2 of the model to compare it with that of the
217 near-continental parameterization dataset. We then analyzed the occurrences of regime shifts
218 from forest to savanna due to climate change and deforestation on a grid of cells representing
219 the study area. This grid had the resolution of the precipitation data (0.5°). We considered
220 spatial interactions (e.g. dispersion of trees) irrelevant on this scale. We resampled the tree-
221 cover data from 0.01° to 0.5° resolution using the ArcGIS ‘majority’ resampling method. This
222 method of resampling encompasses assigning the value to the output cell that is most
223 abundant in the input cells. We assumed that the 2500 input cells per output cell are sufficient

to distinguish between the savanna, forest and treeless states. The choice for 'majority' prevents a bias towards average, unrealistic tree-cover values. For reasons of convenience, the resampled tree cover is called 'observed' in this paper. We ran the model with those observed values as initial conditions and imposed climate change and deforestation on the cells that have an observed tree cover of at least 0.60 and also stabilized at the forest state in the model.

Gradual climate change was simulated by decreasing MAP with steps of 0.01 times the measured value for each cell. At each step, observed tree cover was set as initial condition. Subsequently, tree cover of forest cells was reduced with steps of 0.01 (up to 0.30) times the observed cover to check when a shift to savanna took place resulting from deforestation. This simulation continued up to a precipitation reduction of 40%, which can be considered as an extreme scenario. The interaction effects of deforestation and drought on the occurrences of regime shifts were quantified as relative increases in the number of cells that shifted to the savanna state. A relative increase was calculated by dividing the total amount of shifted cells at a certain combination of deforestation and precipitation reduction by the amount of cells that had also shifted under either of the two perturbations. All simulations were performed using the GRIND for MATLAB (R2012b) software. Differential equations were solved with the Dormand Prince 4.5 solver (ode45) and all runs consisted of 1000 time steps.

3. Results

The parameterization resulted in a model with three stable tree-cover states: forest ($T \approx 0.85$), savanna ($0.20 \leq T \leq 0.40$) and a treeless state ($T = 0$). Depending on mean annual precipitation, tree cover could be in either of one, two or three possible stable equilibria. Fire intensity starts decreasing sharply after $T \approx 0.40$, causing bistability of forest and savanna for a large precipitation range, from 950 to 2400 mm yr^{-1}. This range is visually in agreement with the continental parameterization data (Fig. 2). The multi-modality in the data was not

249 determined by multi-modality in environmental variables (Appendix A). The precipitation
250 range with bistability is wider than in the model of Van Nes et al. (2014) (1100−1600 mm yr^{-1}
251). This difference results partly from the different parameterizations and partly from the
252 different implementation of the fire-induced tree-cover mortality in the model of this paper
253 (see Appendix D for a more elaborate comparison). The adjusted $R^2_{trimodal}$ of the three means
254 of the regimes was 0.96 and the model's adjusted R^2_{model} was 0.90 (Table S1). In the study
255 area, the R^2_{model} was 0.81 (Table S3).
256 Resampling of the data in the study area did hardly affect the distributions of forest
257 and savanna and the modes in the frequency distribution of tree cover (Fig. A3 and A4; Staver
258 et al., 2011a). When the model was subsequently ran with those resampled data as initial
259 conditions the equilibrium distributions of forest and savanna were consistent with the
260 observations (Fig. 3). By performing model runs after initializing the grid at various tree-
261 cover values (T = 0.85 for forest, 0.30 for savanna and 0.01 for treeless), the geographical
262 range of bistability and tristability could be determined (Fig. A6). In 4% of the cells forest
263 was the only stable state. These cells were located in the state of Amazonas (in the block 5-
264 −6.5°S and 71−65.5°W), at the border of the states of Amazonas, Pará and Mato Grosso
265 (7−8°S and 58.5−57.5°W) and in Peru near the Bolivian border (11−14°S and 71−69°W). In
266 the remaining cells savanna was stable. Also, tree cover remained at the forest state in 94% of
267 the cells, implying bistability of forest and savanna in 90% of the cells. This area extends as
268 east as Piauí (approximately 44°W longitude). Tree cover decreased to a treeless state (T <
269 0.001) in 13% of the cells. Thus, in 7% the cells tree cover stabilized at another state in all
270 three runs.
271

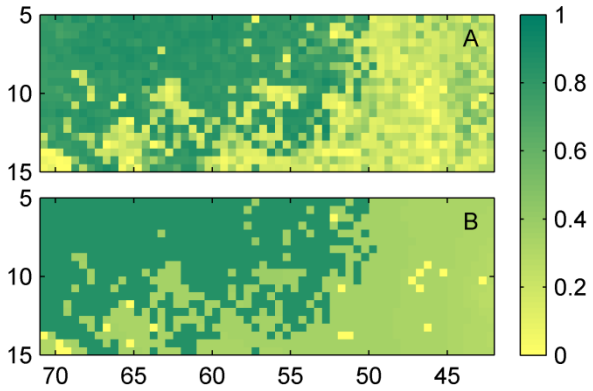

Figure 3: Tree cover in the study area at 0.5° resolution. A) Observed tree cover; and B) tree cover after stabilization in the model with the observed tree cover as initial conditions.

Reducing MAP in the cells with observed forest resulted in critical transitions to savanna (Fig. 4). At the most extreme scenario considered (40% reduction in MAP), 19% of the forested cells had shifted to savanna. A similar amount of cells (22%) had shifted in the absence of climate change at a deforestation of 20% tree cover per cell (Fig. 4). More than half of the forest (281 cells, being 51%) disappeared when 30% of the observed tree cover was subtracted from each cell. In combination, drought and deforestation tipped forested cells to the savanna state at lower levels of these perturbations than by themselves. Furthermore, more cells underwent a regime shift in the simulated ranges of the perturbations (Fig. 4). This interactive effect was most pronounced when precipitation reduction was between 20−40% and deforestation between 10−20%, when, on average, five times as many cells shifted than at the respective precipitation reduction and deforestation separately (Fig. A7). The largest interaction effect was found at a reduced MAP of 32% and deforestation of 14% at each cell, when 6.6 times as many shifts were observed.

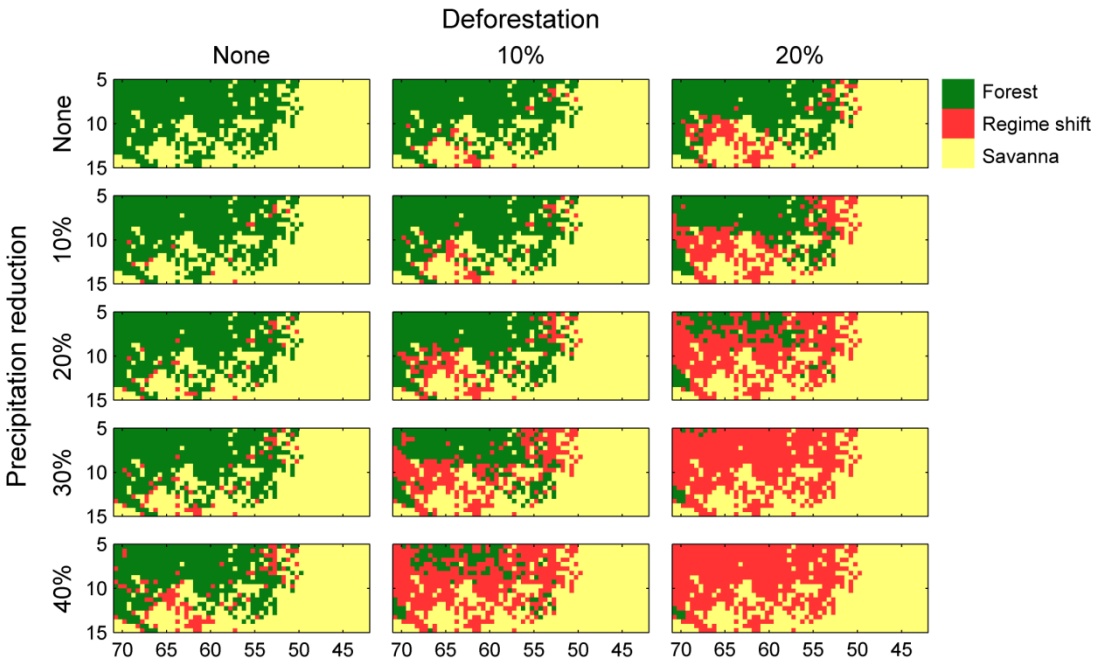

Figure 4: Regime shifts from forest to savanna at different levels of precipitation reduction and deforestation. The rows represent situations without precipitation reduction and with 10%, 20%, 30% and 40% reduction of current mean annual precipitation. The columns represent situations without deforestation and with removal of 10% and 20% of the observed tree cover. Green cells indicate locations where forest is predicted under the given conditions (MODIS tree cover without human-used areas excluded). Red cells indicate a predicted regime shift to a savanna ecosystem and light-yellow cells are already in a savanna (or treeless) regime.

4. Discussion

We presented a simple model that has three alternative tree-cover states and was fitted on tree-cover data from tropical and sub-tropical South America. Due to a simple tree cover-fire feedback depending on climate the model has bistability of forest and savanna over a large range of mean annual precipitation (950−2400 mm yr^{-1}). Our analysis using tree-cover and precipitation data from the south-eastern Amazon rainforest suggests a strong synergy

306 between drought and deforestation on the occurrence of regime shifts in this area. Drought,
307 simulated as a reduction in mean annual precipitation (MAP), decreased the resilience of the
308 forest state, thereby increasing the chance that a perturbation such as deforestation causes a
309 shift to a savanna regime. Similarly, a perturbed forest was more likely to undergo a regime
310 shift as a result of drought. Deforestation and drought interacted strongly because both
311 increased fire intensity. How this interaction caused regime shifts is illustrated in Fig. 5,
312 where a hypothesized combination of deforestation and drought pushes the system to the
313 savanna basin of attraction. Separately, neither of the two would cause such a shift, due to the
314 shape of the unstable equilibrium line. The synergy was strongest around 30−35%
315 precipitation reduction and 15% deforestation, where the interaction effect accounted for over
316 80% of the regime shifts. This suggests that plausible levels of either deforestation or
317 precipitation reduction could strongly increase the sensitivity of the south-eastern Amazon
318 rainforest to the other if an unstable threshold is approached (Van Nes and Scheffer, 2003).
319 However, most forest cells may undergo a shift due to deforestation even in the absence of a
320 change in MAP, because they were bi- or tristable. On the other hand, in many cells a critical
321 transition due to precipitation reduction occurred only in combination with deforestation,
322 despite the finding that the forest may already be out of equilibrium.
323

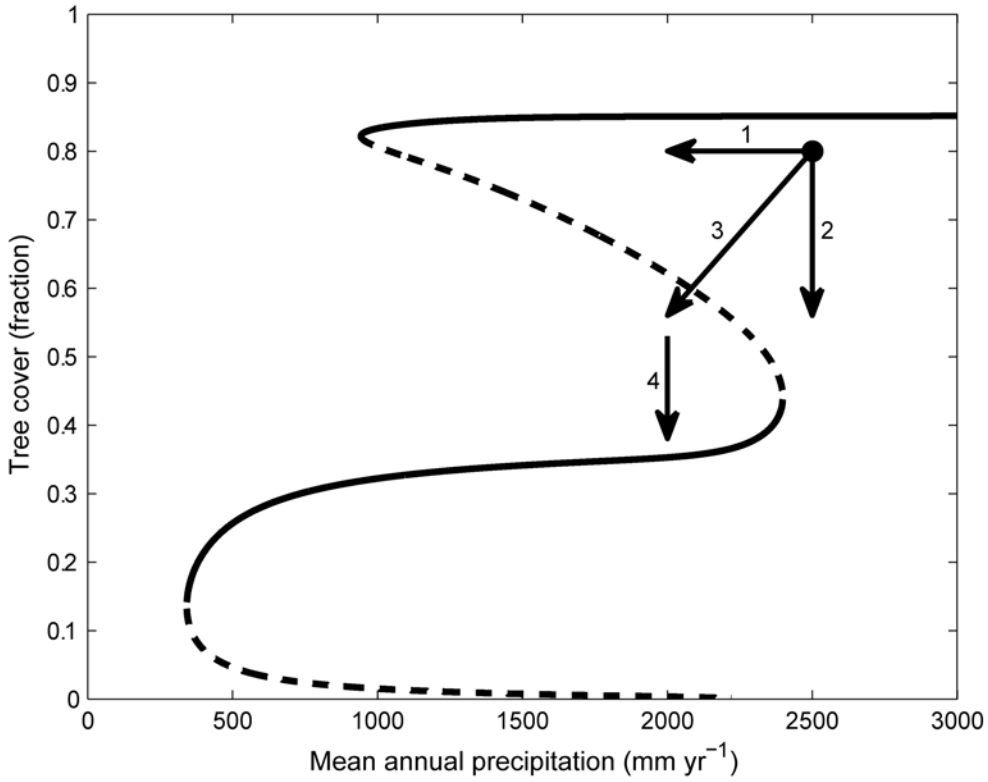

Figure 5: How the interaction between precipitation reduction and deforestation may cause a regime shift in the model. If in a forested area with $T = 0.80$ at $P = 2500$ mm yr^{-1} a decrease in precipitation of 20% takes place (1), no changes in the state of the system would be apparent, as the system is still in the basin of attraction of the forest state. However, savanna has become an alternate stable state, so a simultaneous deforestation of 30% (2) may push the system across the unstable equilibrium (3). The system then moves to the savanna state (4). Note that the position of a site relative to the unstable equilibrium line in the model determines at which combinations of precipitation reduction and deforestation the system undergoes regime shifts.

The modeled relationship between tree cover and fire intensity agrees with the empirical findings of Archibald et al. (2009) that fire becomes rare when tree cover exceeds 0.40. Thus, this feedback mechanism could plausibly cause the apparent forest-savanna bistability as

observed by Hirota et al. (2011) and Staver et al. (2011b). We were able to reproduce the statistical patterns of tree cover in South America, although we ignored factors such as the different response of savanna- and forest-tree species to fire. Nevertheless, this difference in response to fire is known to be an important factor in savanna dynamics (Hoffmann et al., 2012). Forest trees have much higher mortality rates in response to fire than savanna trees, but also have a competitive advantage over savanna trees under shaded conditions (Hoffmann et al., 2012). These differences between the functional types have been included in a simple model by Staver and Levin (2012). The same principle can be included in our model by adding a tree-cover equation for each of the two functional types. Such an addition could help incorporating tree-cover hysteresis in Dynamic Global Vegetation Models (DGVMs) that differentiate between these functional types. Often, such DGVMs insufficiently account for the tree cover-fire feedback (Baudena et al., 2014). One difficulty in parameterizing for various functional types in our type of model lies, however, in the fact that the tree-cover data aggregate all tree species. Essentially, only the percentage of area covered by woody species (tree cover) and the area covered by herbaceous species (1 – tree cover) can be obtained. This is a limitation that causes a need for studies that relate tree-cover data to other biologically relevant variables. Recently, Yin et al. (2014) showed for West-Africa that the tree-cover bimodality coincides with aboveground biomass bimodality and inferred vegetation structure from these results. The low tree-cover mode had low biomass and consisted of savanna species (vertical structure) as well as of forest species (horizontal structure). The high tree-cover mode only consisted of forest species, but could have either high or low biomass (Yin et al., 2014).

We checked whether the bimodality in the tree-cover distribution could be explained by bimodality in annual temperature or precipitation, but this was not the case. Staver et al. (2011b) found, however, that at very strong rainfall seasonality forests are rarely found. This

363 is relevant, as an increase in dry-season length is expected for the south-eastern Amazon that
364 may have profound effects on the forest (Fu et al., 2013). However, because savannas can be
365 found in the tropics regardless of dry-season length (Staver et al., 2011b), weak seasonality
366 would not prevent the regime shifts that our model predicts. Nevertheless, the inclusion of
367 seasonality, as well as inter-annual precipitation variability (Holmgren et al., 2013), may be
368 an interesting option for future explorations of the model.

369 Some possible biases in the data deserve mentioning. Firstly, a bias in the tree-cover
370 data may lie in the algorithms used to generate the MODIS data. As Hanan et al. (2014) show,
371 uniformly distributed tree cover may be reflected in an increased frequency of tree cover in
372 the savanna range. We did not correct for this, and apart from excluding human-used areas
373 used the same dataset as Hirota et al. (2011). Secondly, the hysteresis inferred by Staver et al.
374 (2011b) and this study may be overestimated, as the large hysteresis suggested by the data
375 may also be a manifestation of a range of smaller hysteresis loops resulting from
376 heterogeneity in the landscape (e.g. regarding the soil; Van Nes et al., 2014). On the other
377 hand, we did not consider any feedbacks in the climate, which may increase the bistability
378 range. Although the exact relation between deforestation and precipitation is complex
379 (Lawrence and Vandecar, 2015), we can expect that the regional positive forest-precipitation
380 feedback in the Amazon (Oyama and Nobre, 2003; Zemp et al., 2014) would contribute to a
381 deforestation-triggered transition to savanna. Because of such cross-scale interactions, linking
382 feedbacks across scales would increase our understanding of the resilience of the system at
383 landscape scale (Rietkerk et al., 2011).

384 In our model, the unstable threshold between the basins of attraction of forest and
385 savanna that we attribute to fire is climate-dependent: at higher levels of MAP the resilience
386 of the forest biome increases due to decreased fire intensity. Thus we provide regarding South
387 America a more refined value for this threshold than Hirota et al. (2011), who suggested a

388 climate-insensitive unstable equilibrium at 60% tree cover. A climate-dependent unstable
389 equilibrium accounts for interaction effects between precipitation reduction and deforestation
390 on regime shifts. Hence, future modeling studies seeking a simple way to include the effects
391 of possible local alternative stable states in Amazonian tree cover could benefit from the
392 approach described here and in Van Nes et al. (2014). On a more applied level, our model
393 predicts that deforestation in the south-eastern Amazon rainforest will result in regime shifts
394 to savanna. Furthermore, degradation of the forest may cause it to become very vulnerable to
395 anthropogenic climate change. Therefore, we endorse the need for policies that counteract
396 deforestation in order to preserve the Amazon rainforest in a world under climate change.
397
398 **Acknowledgements** AS is supported by a PhD scholarship "Complex dynamics in human-
399 environment systems" from SENSE Research School and EHvN is supported by an ERC
400 grant that was awarded to Marten Scheffer. AS is grateful to Rafael Bernardi for his help on
401 processing GLC2000 data and to Sebastian Bathiany for the display of an inspiring
402 acknowledgement.
403

404 References
405
406 Aragão, L.E.O.C., Malhi, Y., Roman-Cuesta, R.M., Saatchi, S., Anderson, L.O.,
407 Shimabukuro, Y.E., 2007. Spatial patterns and fire response of recent Amazonian droughts.
408 Geophysical Research Letters 34, L07701.

409 Archibald, S., Roy, D.P., van Wilgen, B.W., Scholes, R.J., 2009. What limits fire? An
410 examination of drivers of burnt area in Southern Africa. Global Change Biology 15, 613-630.

411 Baudena, M., D'Andrea, F., Provenzale, A., 2010. An idealized model for tree–grass
412 coexistence in savannas: the role of life stage structure and fire disturbances. Journal of
413 Ecology 98, 74-80.

414 Baudena, M., Dekker, S.C., van Bodegom, P.M., Cuesta, B., Higgings, S.I., Lehsten, V.,
415 Reick, C.H., Rietkerk, M., Scheiter, S., Yin, Z., Zavala, M.A., Brovkin, V., 2014. Forests,
416 savannas and grasslands: bridging the knowledge gap between ecology and Dynamic Global
417 Vegetation Models. Biogeosciences Discussions 11, 9471-9510.

418 Bond, W.J., 2008. What limits trees in C4 grasslands and savannas? Annual Review of
419 Ecology, Evolution, and Systematics 39, 641-659.

420 Brando, P.M., Balch, J.K., Nepstad, D.C., Morton, D.C., Putz, F.E., Coe, M.T., Silvério, D.,
421 Macedo, M.N., Davidson, E.A., Nóbrega, C.C., Alencar, A., Soares-Filho, B.S., 2014. Abrupt
422 increases in Amazonian tree mortality due to drought–fire interactions. Proceedings of the
423 National Academy of Sciences 111, 6347-6352.

424 Bucini, G., Hanan, N.P., 2007. A continental-scale analysis of tree cover in African savannas.
425 Global Ecology and Biogeography 16, 593-605.

426 Cochrane, M.A., Alencar, A., Schulze, M.D., Souza Jr, C.M., Nepstad, D.C., Lefebvre, P.,
427 Davidson, E.A., 1999. Positive feedbacks in the fire dynamic of closed canopy tropical
428 forests. Science 284, 1832-1835.

429 Coe, M.T., Marthews, T.R., Costa, M.H., Galbraith, D.R., Greenglass, N.L., Imbuzeiro,
430 H.M.A., Levine, N.M., Malhi, Y., Moorcroft, P.R., Muza, M.N., Powell, T.L., Saleska, S.R.,
431 Solorzano, L.A., Wang, J., 2013. Deforestation and climate feedbacks threaten the ecological
432 integrity of south-southeastern Amazonia. Philosophical Transactions of the Royal Society B:
433 Biological Sciences 368, 20120155.

434 Cox, P.M., Betts, R.A., Jones, C.D., Spall, S.A., Totterdell, I.J., 2000. Acceleration of global
435 warming due to carbon-cycle feedbacks in a coupled climate model. Nature 408, 184-187.

436 Cumming, G.S., Southworth, J., Rondon, X.J., Marsik, M., 2012. Spatial complexity in
437 fragmenting Amazonian rainforests: Do feedbacks from edge effects push forests towards an
438 ecological threshold? Ecological Complexity 11, 67-74.

439 Davidson, E.A., De Araüjo, A.C., Artaxo, P., Balch, J.K., Brown, I.F., C. Bustamante, M.M.,
440 Coe, M.T., Defries, R.S., Keller, M., Longo, M., Munger, J.W., Schroeder, W., Soares-Filho,
441 B.S., Souza Jr, C.M., Wofsy, S.C., 2012. The Amazon basin in transition. Nature 481, 321-
442 328.

443 Farr, T.G., Rosen, P.A., Caro, E., Crippen, R., Duren, R., Hensley, S., Kobrick, M., Paller,
444 M., Rodriguez, E., Roth, L., 2007. The shuttle radar topography mission. Reviews of
445 Geophysics 45, RG2004.

446 Fu, R., Yin, L., Li, W., Arias, P.A., Dickinson, R.E., Huang, L., Chakraborty, S., Fernandes,
447 K., Liebmann, B., Fisher, R., Myneni, R.B., 2013. Increased dry-season length over southern
448 Amazonia in recent decades and its implication for future climate projection. Proceedings of
449 the National Academy of Sciences 110, 18110-18115.

450 Gil-Romera, G., Lamb, H.F., Turton, D., Sevilla-Callejo, M., Umer, M., 2010. Long-term
451 resilience, bush encroachment patterns and local knowledge in a Northeast African savanna.
452 Global environmental change 20, 612-626.

453 Hanan, N.P., Tredennick, A.T., Prihodko, L., Bucini, G., Dohn, J., 2014. Analysis of stable
454 states in global savannas: is the CART pulling the horse? Global Ecology and Biogeography
455 23, 259-263.

456 Hansen, M., DeFries, R., Townshend, J., Carroll, M., Dimiceli, C., Sohlberg, R., 2003. Global
457 percent tree cover at a spatial resolution of 500 meters: First results of the MODIS vegetation
458 continuous fields algorithm. Earth Interactions 7, 1-15.

459 Hirota, M., Holmgren, M., Van Nes, E.H., Scheffer, M., 2011. Global resilience of tropical
460 forest and savanna to critical transitions. Science 334, 232-235.

461 Hirota, M., Nobre, C., Oyama, M.D., Bustamante, M.M.C., 2010. The climatic sensitivity of
462 the forest, savanna and forest-savanna transition in tropical South America. New Phytologist
463 187, 707-719.

464 Hoffmann, W.A., Geiger, E.L., Gotsch, S.G., Rossatto, D.R., Silva, L.C., Lau, O.L.,
465 Haridasan, M., Franco, A.C., 2012. Ecological thresholds at the savanna-forest boundary:

how plant traits, resources and fire govern the distribution of tropical biomes. Ecology Letters 15, 759-768.

Holling, C.S., 1973. Resilience and stability of ecological systems. Annual Review of Ecology and Systematics 4, 1-23.

Holmgren, M., Hirota, M., Van Nes, E.H., Scheffer, M., 2013. Effects of interannual climate variability on tropical tree cover. Nature Climate Change 3, 755-758.

Holmgren, M., Scheffer, M., Huston, M.A., 1997. The interplay of facilitation and competition in plant communities. Ecology 78, 1966-1975.

Lawrence, D., Vandecar, K., 2015. Effects of tropical deforestation on climate and agriculture. Nature Climate Change 5, 27-36.

Lenton, T.M., Held, H., Kriegler, E., Hall, J.W., Lucht, W., Rahmstorf, S., Schellnhuber, H.J., 2008. Tipping elements in the Earth's climate system. Proceedings of the National Academy of Sciences 105, 1786-1793.

Malhi, Y., Aragão, L.E.O.C., Galbraith, D., Huntingford, C., Fisher, R., Zelazowski, P., Sitch, S., McSweeney, C., Meir, P., 2009. Exploring the likelihood and mechanism of a climate-change-induced dieback of the Amazon rainforest. Proceedings of the National Academy of Sciences 106, 20610-20615.

Malhi, Y., Roberts, J.T., Betts, R.A., Killeen, T.J., Li, W., Nobre, C.A., 2008. Climate change, deforestation, and the fate of the Amazon. Science 319, 169-172.

485 Mitchell, T.D., Jones, P.D., 2005. An improved method of constructing a database of monthly
486 climate observations and associated high-resolution grids. International Journal of
487 Climatology 25, 693-712.

488 Moreira, A.G., 2000. Effects of fire protection on savanna structure in central Brazil. Journal
489 of Biogeography 27, 1021-1029.

490 Murphy, B.P., Bowman, D.M.J.S., 2012. What controls the distribution of tropical forest and
491 savanna? Ecology Letters 15, 748-758.

492 Nepstad, D.C., Stickler, C.M., Soares-Filho, B., Merry, F., 2008. Interactions among Amazon
493 land use, forests and climate: Prospects for a near-term forest tipping point. Philosophical
494 Transactions of the Royal Society B: Biological Sciences 363, 1737-1746.

495 Nobre, C.A., Borma, L.D.S., 2009. 'Tipping points' for the Amazon forest. Current Opinion in
496 Environmental Sustainability 1, 28-36.

497 Oyama, M.D., Nobre, C.A., 2003. A new climate-vegetation equilibrium state for tropical
498 South America. Geophysical Research Letters 30, 2199.

499 Pueyo, S., de Alencastro Graça, P.M.L., Barbosa, R.I., Cots, R., Cardona, E., Fearnside, P.M.,
500 2010. Testing for criticality in ecosystem dynamics: The case of Amazonian rainforest and
501 savanna fire. Ecology Letters 13, 793-802.

502 Ratter, J.A., 1992. Transitions between cerrado and forest vegetation in Brazil, in: Furley,
503 P.A., Proctor, A., Ratter, J.A. (Eds.), Nature and dynamics of forest-savanna boundaries.
504 Chapman and Hall, London, pp. 417-429.

505 Reyer, C.P.O., Brouwers, N., Rammig, A., Brook, B.W., Epila, J., Grant, R.F., Holmgren, M.,
506 Langerwisch, F., Leuzinger, S., Lucht, W., Medlyn, B., Pfeifer, M., Steinkamp, J.,
507 Vanderwel, M.C., Verbeeck, H., Villela, D.M., 2015. Forest resilience and tipping points at
508 different spatio-temporal scales: approaches and challenges. Journal of Ecology 103, 5-15.

509 Rietkerk, M., Brovkin, V., van Bodegom, P.M., Claussen, M., Dekker, S.C., Dijkstra, H.A.,
510 Goryachkin, S.V., Kabat, P., van Nes, E.H., Neutel, A.M., Nicholson, S.E., Nobre, C.,
511 Petoukhov, V., Provenzale, A., Scheffer, M., Seneviratne, S.I., 2011. Local ecosystem
512 feedbacks and critical transitions in the climate. Ecological Complexity 8, 223-228.

513 Sankaran, M., Hanan, N.P., Scholes, R.J., Ratnam, J., Augustine, D.J., Cade, B.S., Gignoux,
514 J., Higgins, S.I., Le Roux, X., Ludwig, F., Ardo, J., Banyikwa, F., Bronn, A., Bucini, G.,
515 Caylor, K.K., Coughenour, M.B., Diouf, A., Ekaya, W., Feral, C.J., February, E.C., Frost,
516 P.G.H., Hiernaux, P., Hrabar, H., Metzger, K.L., Prins, H.H.T., Ringrose, S., Sea, W., Tews,
517 J., Worden, J., Zambatis, N., 2005. Determinants of woody cover in African savannas. Nature
518 438, 846-849.

519 Scheffer, M., 2009. Critical Transitions in Nature and Society. Princeton University Press,
520 Princeton.

521 Scheffer, M., Bascompte, J., Brock, W.A., Brovkin, V., Carpenter, S.R., Dakos, V., Held, H.,
522 Van Nes, E.H., Rietkerk, M., Sugihara, G., 2009. Early-warning signals for critical
523 transitions. Nature 461, 53-59.

524 Scheffer, M., Carpenter, S.R., 2003. Catastrophic regime shifts in ecosystems: Linking theory
525 to observation. Trends in Ecology and Evolution 18, 648-656.

526 Scheffer, M., Hirota, M., Holmgren, M., Van Nes, E.H., Chapin Iii, F.S., 2012. Thresholds for
527 boreal biome transitions. Proceedings of the National Academy of Sciences 109, 21384-
528 21389.

529 Staver, A.C., Archibald, S., Levin, S., 2011a. Tree cover in sub-Saharan Africa: rainfall and
530 fire constrain forest and savanna as alternative stable states. Ecology 92, 1063-1072.

531 Staver, A.C., Archibald, S., Levin, S.A., 2011b. The global extent and determinants of
532 savanna and forest as alternative biome states. Science 334, 230-232.

533 Staver, A.C., Levin, S.A., 2012. Integrating theoretical climate and fire effects on savanna and
534 forest systems. The American Naturalist 180, 211-224.

535 Sternberg, L.S.L., 2001. Savanna-forest hysteresis in the tropics. Global Ecology and
536 Biogeography 10, 369-378.

537 Uhl, C., Kauffman, J.B., 1990. Deforestation, fire susceptibility, and potential tree responses
538 to fire in the eastern Amazon. Ecology 71, 437-449.

539 Van Nes, E.H., Hirota, M., Holmgren, M., Scheffer, M., 2014. Tipping points in tropical tree
540 cover: linking theory to data. Global Change Biology 20, 1016-1021.

541 Van Nes, E.H., Holmgren, M., Hirota, M., Scheffer, M., 2012. Response to comment on
542 "Global resilience of tropical forest and savanna to critical transitions". Science 336, 541-d.

543 Van Nes, E.H., Scheffer, M., 2003. Alternative attractors may boost uncertainty and
544 sensitivity in ecological models. Ecological Modelling 159, 117-124.

545 Yin, Z., Dekker, S., van den Hurk, B., Dijkstra, H., 2014. Bimodality of woody cover and
546 biomass across the precipitation gradient in West Africa. Earth System Dynamics 5, 257-270.

547 Zemp, D.C., Schleussner, C.F., Barbosa, H.M.J., van der Ent, R.J., Donges, J.F., Heinke, J.,
548 Sampaio, G., Rammig, A., 2014. On the importance of cascading moisture recycling in South
549 America. Atmospheric Chemistry and Physics 14, 13337-13359.
550

Appendix A. Trimodal tree cover and the model's goodness-of-fit

The frequency distribution of tree cover in tropical and subtropical South America (13°N−35°S; excluding human-used areas) is trimodal (Fig. A1).

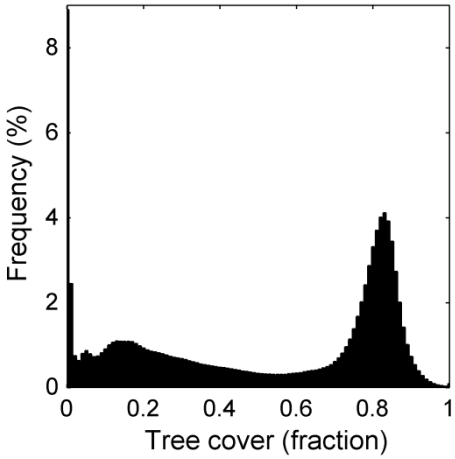

Fig. A1: The frequency distribution of the tree-cover data used for parameterizing the model (n = 9293107).

Fig. A2 shows that the trimodality in tree cover does not result from multimodality in mean annual precipitation (MAP) and mean annual temperature. Data points were divided into treeless, savanna and forest based on the minima of the frequency distribution of tree cover. These were 0.04 and 0.56 (Fig. A1), so the three groups (or regimes) were determined as $0 \leq T \leq 0.04$ (treeless), $0.05 \leq T \leq 0.56$ (savanna) and $0.57 \leq T \leq 1$ (forest). The mean annual temperature for each 0.5° cell in the study area was determined by averaging monthly Climate Research Unit data from 1960−2000 (Mitchell and Jones, 2005). The cells were reshaped to 0.01° in MATLAB R2012b.

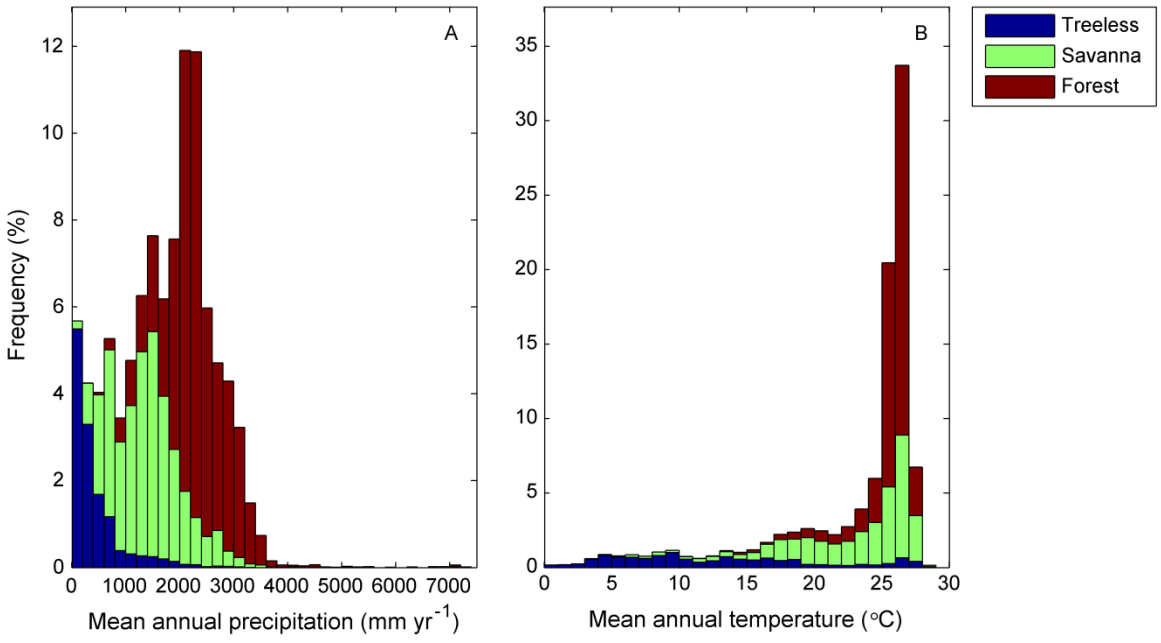

Fig. A2: Histograms of mean annual precipitation (A) and mean annual temperature (B) in tropical and subtropical South America with the distribution of treeless, savanna and forest regimes indicated.

We ran the model for five samples of 1000 data points until equilibrium. We then determined the deviations of the initial values (MODIS observations) to the stable outcomes of the run. We computed for each sample the adjusted R^2, whereby we adjusted for the seven fitted parameters in the model (α, β, γ, FRI, h_C, h_I and h_P). However, to estimate the goodness-of-fit to a trimodal tree-cover distribution we wanted to compare the adjusted R^2_{model} to that of an 'optimal model' with three possible predictions. Therefore, we also calculated the $R^2_{trimodal}$ of the means of the three regimes, again where $0 \leq T \leq 0.04$ was treeless, $0.05 \leq T \leq 0.56$ savanna and $0.57 \leq T \leq 1$ was considered forest. We adjusted $R^2_{trimodal}$ for the three means. The average $R^2_{trimodal}$ of the samples (R^2 = 0.96) was higher than the average R^2_{model} (R^2 = 0.90) (Table A1).

Table A1: The adjusted $R^2_{trimodal}$ of the means of the three modes to sampled data points (five independent sample of 1000) and the adjusted R^2_{model} of the model to those data points. Values in boldface are averages.

Sample	Adj. $R^2_{trimodal}$	Adj. R^2_{model}
1	0.964	0.897
2	0.962	0.908
3	0.963	0.909
4	0.963	0.888
5	0.963	0.900
	0.963	**0.900**

Appendix B. Data from the study area

The frequency distribution of the tree cover data (at 0.01° resolution; Hirota et al., 2011) in the study area has two clear modes for savanna (T = 0.17) and forest (T = 0.83) as well as a small one for treeless (T = 0) (Fig. B1A). The minima between these modes are at T = 0.03 and T = 0.64. Resampling hardly affects the positioning and shape of the modes (Staver et al., 2011a). After converting the cells from 0.01° to 0.5° in which each 0.5° cell was given the most frequently occurring value out of 2500 cells at 0.01°, modes were located at T = 0.17 and T = 0.81; T = 0 is not present after resampling (Fig. B1B). Of the resampled cells, 1% (14 out of a total of 1160) was entirely treeless, 51% (587 in total) had tree cover up to 0.60 and 48% (559) were forested. Both before and after resampling, forest was found to exist mainly in areas with MAP > 1300 mm yr^{-1}. Savanna is present up until about 2300 mm yr^{-1} (Fig. B2).

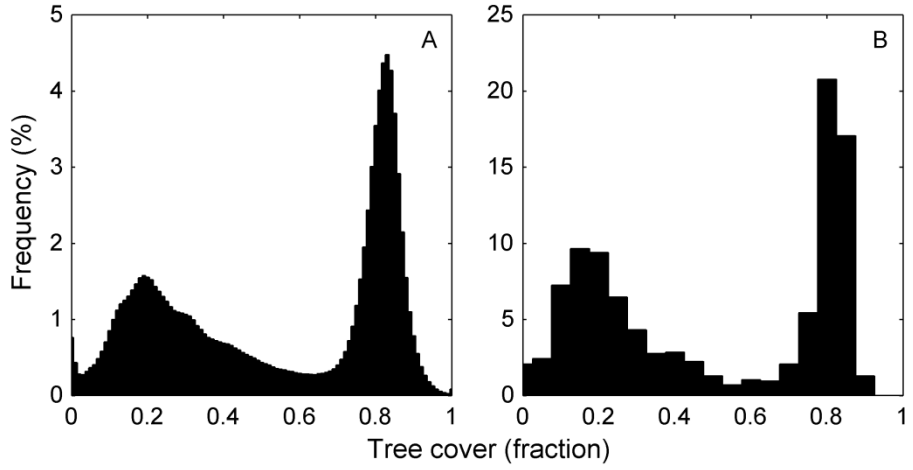

Fig. B1: Histograms of tree cover in the study area at (A) 0.01° resolution; and (B) after resampling to 0.5° resolution.

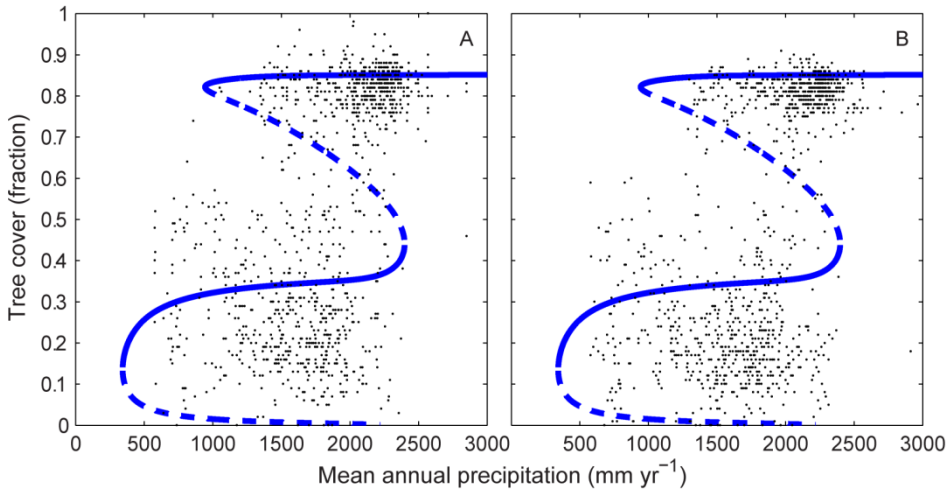

Fig. B2: Stable (solid lines) and unstable (dashed lines) equilibria with (A) a sample of 1152 data points at 0.01° resolution from the study area; and (B) with all 1152 resampled data points from the study area in the MAP range 0–3000 mm yr^{-1}.

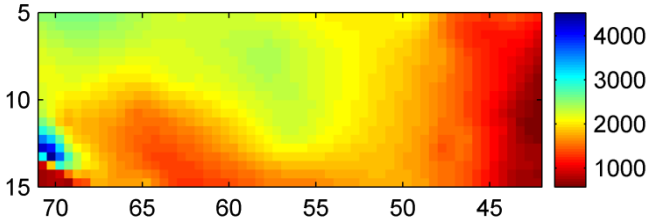

Fig. B3: Mean annual precipitation (mm yr^{-1}) in the study area.

We checked how tree cover in the study area relates to environmental variables. Besides MAP (Fig. B3) and temperature, we considered landscape elevation. Elevation data taken from the NASA Shuttle Radar Topography Mission (Farr et al., 2007). These data are at 3 arcsecond resolution and were therefore averaged to 0.01° (i.e. 144 values were averaged to one). Any missing values in the original data were ignored. Regressions between these variables were performed in SPSS 21 with five independent samples of 1000 data points. MAP is strongly correlated to tree cover (R^2 = 0.31). Elevation is moderately negatively correlated to tree

cover (R^2 = 0.09) and mean annual temperature is weakly correlated to tree cover (R^2 = 0.03) (Table B1).

Table B1: Pearson's R^2 between elevation, mean annual temperature, mean annual precipitation and tree cover for the study area at 0.01° resolution. The results are of samples of 1000 out of 2872105 data points (681984 for correlations with elevation) and are highly significant (p << 0.01). Values in boldface are averages.

	Temperature	Precipitation	Tree cover
Elevation	0.874	0.139	0.077
	0.878	0.125	0.088
	0.895	0.149	0.105
	0.857	0.142	0.076
	0.803	0.144	0.092
	0.861	**0.140**	**0.088**
Temperature		0.031	0.030
		0.038	0.027
		0.043	0.032
		0.028	0.033
		0.016	0.014
		0.031	**0.027**
Precipitation			0.350
			0.291
			0.292
			0.334
			0.274
			0.308

Appendix C. Stability of tree cover in the study area

We also calculated the adjusted R^2_{model} in the study area (Table C1). The average of five samples is R^2 = 0.81, which is lower than in the parameterization dataset (R^2 = 0.90).

Table C1: The adjusted R^2_{model} of the model to sampled data points (five independent sample of 1000) from the study area. The values in boldface is an average.

Sample	Adj. R^2_{model}
1	0.793
2	0.821
3	0.828
4	0.802
5	0.815
	0.812

Fig. C1 shows the distribution of the three ecosystem states in the study area after initializing the entire grid at: 1) forest (T = 0.85); 2) savanna (T = 0.30); and 3) treeless (T = 0.01).

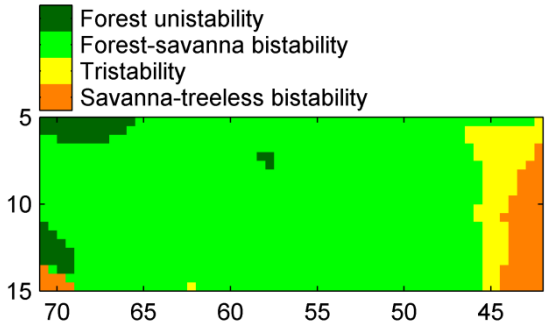

Fig. C1: Stable states after different tree cover initializations.

The interaction effect between deforestation and precipitation reduction was quantified as the relative increase in the number of regime shifts at a certain combination of the two compared to the number of shifts at deforestation and precipitation reduction separately. Fig. C2 visualizes how this interaction effect depends on the extent of precipitation reduction and deforestation for the 547 forest cells (0.5° resolution) in the study area.

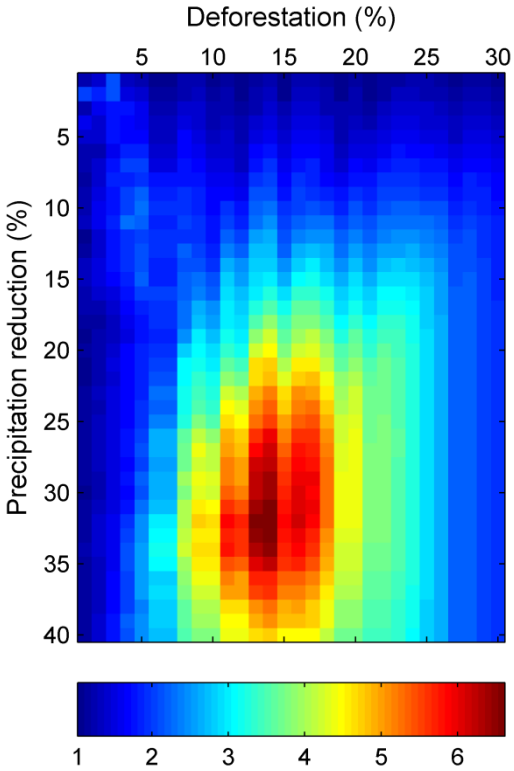

Fig. C2: The interaction effect between deforestation and precipitation reduction on the occurrence of regime shifts in the study area. The numbers indicate the relative increase in the number of regime shifts compared to the number of shifts at the respective deforestation and precipitation reduction separately.

Appendix D. Comparison with the Van Nes et al. (2014) model

Using the names and abbreviations of the parameters and variables from this paper, the Van Nes et al. (2014) model can be phrased as follows:

$$\frac{dT}{dt} = \frac{P}{h_P+P}\, r_m\, T\, \left(1-\frac{T}{K}\right) - m_A\, T\, \frac{h_A}{T+h_A} - T\, \frac{1}{FRI}\, \frac{{h_C}^{\beta}}{{h_C}^{\beta}+T^{\beta}} \quad \text{(D1)}$$

and in its original form is parameterized as in Table D1.

Table D1: Parameterization of Van Nes et al. (2014). For comparison, the names, descriptions and units of this paper are retained.

Parameter	Description	Value	Unit
β	Power in continuity function	7	None
FRI	Fire return interval	1 / 0.11	yr
h_A	Half saturation of Allee effect	0.10	Fractional tree cover
h_C	Half saturation of grass (non-forest) cover continuity	0.64	Fractional tree cover
h_P	Half saturation of growth term	182.5	mm yr^{-1}
K	Maximum tree cover	0.90	Fractional tree cover
m_A	Mortality due to Allee effect	0.15	yr^{-1}
r_m	Maximum tree-cover growth rate	0.30	yr^{-1}

The forest-savanna hysteresis of the Van Nes et al. (2014) model is 1100−1600 mm yr^{-1}, smaller than of the paper presented in this paper (Fig. D1). When the Van Nes et al. (2014) model is parameterized as Table 1 (i.e. the fire-induced mortality only depends on *T*) it has a bistability range of 350−1500 mm yr^{-1} (with forest also stable between 250−350 mm yr^{-1}). If this fire mortality term is multiplied by the soil moisture index, tree-cover mortality due to fire effectively equals annual fire intensity times tree cover. Performing this multiplication results in a bistability range of 350−850 mm yr^{-1}.In the eventual model, tree cover is made resistant to low-intensity fires by incorporating a Hill function. Because this Hill function allows fire-induced tree-cover mortality to approach 1 (divided by *FRI*) when intensity is considerably larger than half saturation h_I, higher mortality is possible than without this function. When the exponent γ is set to 1, tree cover increases with MAP without forest and savanna being alternative stable states. Bistability and hysteresis arise when γ exceeds approximately 1.34 (a fold bifurcation appears at 2040 mm yr^{-1}). At higher γ hysteresis widens, with a forest-savanna bistability at 950−2400 mm yr^{-1} at $\gamma = 6$.

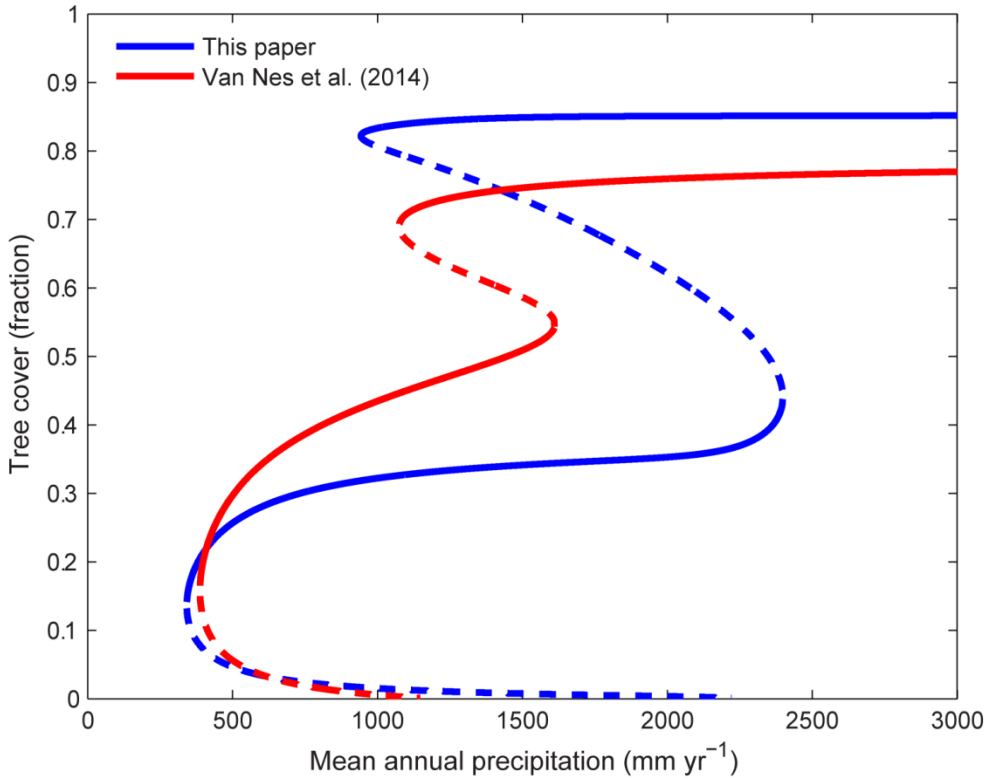

Fig. D1: The stable (solid lines) and unstable (dashed lines) tree-cover equilibria of the model presented in this paper and in Van Nes et al. (2014).

Appendix E. Sensitivity analysis of the model

With a sensitivity analysis on the parameters it is observed how strongly the precipitation range at which both forest and savanna are stable is affected. Largest sensitivity was found on h_c and K, lowest on h_p (Table E1).

Table E1: Sensitivity analysis of the model, showing the ranges of mean annual precipitation at which forest and savanna are both stable (rounded at 50 mm yr^{-1} and the treeless state not accounted for). At the default parameter settings the bistable range is 950–2400 mm yr^{-1}.

Parameter	Value	-20%	-10%	+10%	+20%
α	4	850-2550	900-2450	1000-2350	1050-2300
β	6	1550-2350	1350-2350	250-2400	150-2450
γ	6	1200-2350	1100-2350	800-2400	650-2450
FRI	7	1050-2550*	1000-2500	900-2300	850-2200
h_A	0.10	750-2350	850-2400	1050-2400	1100-2450
h_c	0.57	50-2150	100-2300	1700-2450	2050-2550
h_I	0.15	1350-2550	1200-2500	550-2300	300-2250
h_{SMI}	1800	800-1900	850-2150	1050-2650	1150-2850
K	0.90	2250-2550	1750-2500	100-2300	50-2150
m_A	0.15	700-2300	850-2350	1050-2400	1150-2450
r_m	0.30	1250-2600**	1100-2500	800-2300	600-2200

* Savanna is only stable above 1500 mm yr^{-1}. ** Savanna is only stable above 2400 mm yr^{-1}.